Conference and Euromech Colloquium #480

on

High Rayleigh Number Convection

4 - 8 Sept., 2006, ICTP, Trieste, Italy

Conference Abstracts

Titles and Abstracts

Directors: D. Lohse and R. Verzicco

These are preliminary lecture notes, intended only for distribution to participants

Conference and Euromech Colloquium #480
on
High Rayleigh Number Convection

4 - 8 Sept., 2006, ICTP, Trieste, Italy

Directors: D. Lohse and R. Verzicco

Conference Abstracts

Titles and Abstracts

1)   Xia, K. Q., (Hong Kong)

Cascades, decoherence and plumes in turbulent thermal convection

2)   Gibert, M. (Lyon)

High Rayleigh number convection in a vertical channel

 We measure the relation between convective heat flux and temperature gradient in a vertical channel filled with water, the average vertical mass flux being zero. Compared to the classical Rayleigh-Bénard case, this situation has the advantage of avoiding plates and, thus, their neighborhood, in which is usually concentrated most of the temperature gradient. Consequently, inertial processes should control the convection, with poor influence of the viscosity. This idea gives a good account of our observations, if we consider that a natural vertical length, different from the channel width, appears. Our results also suggest that heat fluxes can be deduced from velocity measurements in free convective flows. This confers to our results a wide range of applications.

3) Shishkina, O. (Goettingen)

Local heat transport analysis based on DNS/LES of turbulent RBC in wide cylindrical containers

Vertical heat fluxes and thermal dissipation rates in turbulent Rayleigh–Bénard convection, their spatial distributions and some mean characteristics are studied based on data obtained in DNS for Rayleigh numbers $Ra = 10^5$, 10^6 and 10^7 and LES for $Ra = 10^8$ and 10^9 [1–2]. The well resolved LES use the tensor-diffusivity model [3] together with the top-hat filter. In all simulations the Prandlt number $Pr = 0.7$ and the aspect ratios of the cylindrical Rayleigh–Bénard cell $\Gamma = 10$ and 5 are considered.

Analysis of the spatial distribution of the vertical heat flux Ω for any Ra shows that the maximum point of the local heat flux density function coincides with zero. It means that the largest part of the fluid volume corresponds to the local heat flux fluctuating not around the Nusselt number Nu, but around zero. The spread of the tails of the local heat flux distributions depends strongly on the distance from the plates and increases in the bulk. In up to one third of the center horizontal cross-section negative local heat fluxes are found, while at the bottom plate they vary mainly in the interval $0 \leq \Omega < 2Nu$. With growing Ra the zones of the highest values of the time-averaged local heat flux nestle closer to the corners.

Investigation of the spatial distribution of the thermal dissipation rate ε_θ reveals that both the turbulent background part of the domain (i.e. the portion of the whole domain with relatively small ε_θ-values) and the contribution to the volume averaged ε_θ from the turbulent background, increase with Ra. This supports the conjecture by Grossmann and Lohse [5–6] that the background part of the volume averaged thermal dissipation rate increases with Ra .

References

[1] O. Shishkina & C. Wagner. Analysis of thermal dissipation rates in turbulent Rayleigh–Bénard convection. *J. Fluid Mech.*, 546:51–60, 2006.

[2] O. Shishkina & C. Wagner. Local heat fluxes in turbulent Rayleigh–Bénard convection. *Phys. Fluids*, 2006, submitted.

[3] A. Leonard & G. S. Winckelmans. A tensor-diffusivity subgrid model for Large-Eddy Simulation. *Caltech ASCI technical report, cit-asci-tr043*, 043, 1999.

[4] S. Grossmann & D. Lohse. Scaling in thermal convection: a unifying theory. *J. Fluid Mech.*, 407:27–56, 2000.

[5] S. Grossmann & D. Lohse. Fluctuations in turbulent Rayleigh–Bénard convection: The role of plumes. *Phys. Fluids*, 16:4462–4472, 2004.

4) Niemela, J. (Trieste)

High Rayleigh number convection: helium experiments

Various experimental results will be discussed, including those "Made in Italy." Among the latter, we will report measurements* of the Nusselt number, Nu, in turbulent thermal convection in a cylindrical container of aspect ratio 4, where the highest Rayleigh number achieved was $Ra = 2 \times 10^{13}$. Except for the last half a decade or so of Ra, experimental conditions obey the Boussinesq approximation accurately. For these conditions, the data show that the logNu-logRa slope saturates at a value close to 1/3, as observed previously by us in experiments of smaller aspect ratios. The slope over the last half a decade

of Ra is found to increase, as in previous work, although we do not draw conclusions from it because the data fall close to the critical point and the corresponding conditions are likely non-Boussinesq, as will be discussed. We report a modified scaling relation between the plume advection frequency and ${Ra}$ that collapses data for different aspect ratios, as well as the effects of forcing. At high Ra the coherence of the mean wind over the entire container is lost; specifically, the correlation between sensors separated by a diameter vanishes.

*J.J. Niemela and K.R. Sreenivasan, Turbulent convection at high Rayleigh numbers and aspect ratio 4, *J. Fluid Mech.* **557** 411-422 (2006).

5) Fontenele Araujo, F. (Twente)

Prediction of the center temperature for compressible non-Oberbeck-Boussinesq thermal convection

Thermal convection in gaseous ethane at high pressure is theoretically analyzed, focusing on non-Oberbeck-Boussinesq (NOB) effects. On the basis of boundary-layer equations with variable transport properties, it is shown that the top-down symmetry of the velocity, temperature, and density profiles is broken. In particular, we predict that the temperature T_{c} in the center of the convection container is less than the mean temperature $T_{m} = (T_{t} + T_{b})/2$ between the top (T_{t}) and bottom (T_{b}) plates, in contrast to the corresponding NOB effect in classical liquids. We also characterize the temperature profile across the top boundary-layer, as T_{t} approaches the gas-liquid coexistence curve and the corresponding thermal conductivity is enhanced.

6) Sano, M. (Tokyo)

Ultrasonic measurement of mean wind and fluctuations in thermal turbulence of mercury

We report on the measurements of large scale circulation (LSC) and turbulent fluctuations in thermal convection of mercury. Instantaneous velocity profile at 64 to 128 points is directly measured using ultrasonic velocimetry. The structure of LSC and its dynamics are characterized for convection in three different aspect ratio cells, Γ=0.5, 1.0, and 2.0. Energy power spectrum from instantaneous profiles is also obtained. In addition, measurement with multiple transducers is performed to capture the spatio-temporal behavior of the whole structure. Four transducers are implemented, one along the vertical axis of the cylindrical cell, two in the horizontal plane along boundary layer near the top plate, and one movable along vertical direction along the side wall. The analysis of horizontal profile along the boundary layer showed simpler dynamics than the vertical one. We observe propagation of coherent structures along the boundary layer and slow dynamics of rotation of the LSC.

7) Oresta, P. (Bari)

Chaotic behaviour of particles dispersed in a convective turbulent flow

Direct Numerical Simulation and Lagrangian Particle Tracking are carried out to obtain an accurate path of inertial particle randomly dispersed in a convective turbulent flow, confined in a closed, slender, cylindrical domain. Particles mixing in turbulent convective flow shows high inhomogeneity and chaotic behaviour in connection with the velocity fluctuations of the small scale eddies. The chaotic advection of the particle is investigated using the statistical quantities of particles pairs as their average separation and the finite size Lyapunov exponent. In addition, we have tested the sensitivity of the Lagrangian statistics starting from 10^5 until 10^6 particles for three flow regimes, defined by Rayleigh numbers (Ra) Ra=2 10^7, Ra=2 10^8, Ra=2 10^9 and Prandtl number (Pr) Pr=0.7. For these numerical set-up the flow is turbulent, three-dimensional and time dependent. The stochastic Lagrangian results are used to improve the knowledge about pollutant diffusion and the technological innovation of the industrial devices, devoted to decrease the particles deposition or to increase the particles mixing.

8) Busse, F. (Bayreuth)

Understanding turbulence through sequences of bifurcations

The problem of transitions with increasing control parameter from simple to complex forms of flow in homogeneous non-equilibrium fluid systems under steady external conditions is considered. While the first transition in systems that are uniform in two spatial dimensions generically occurs in the form of rolls or stripes, higher transitions reflect the particular physical properties of the system. The latter transitions can be described through numerical analysis and realized in experiments when the bifurcations are supercritical or only weakly subcritical. Their features are of special interest since they often persist as coherent structures in the turbulent states of the respective systems. Examples for transitions up to quaternary bifurcations will be demonstrated in the case of Rayleigh-Bénard convection and will compared with experimental observations and recent numerical simulations of turbulent convection. An experimental movie will be shown.

9) Brown, E. M. (Santa Barbara)

Effect of the Earth's Coriolis force on the large-scale circulation of turbulent Rayleigh-Benard convection

We present measurements of the large-scale circulation (LSC) of turbulent Rayleigh-Bénard convection in water-filled cylindrical samples of heights equal to their diameters. The LSC consists of a single convection cell circulating in a near-vertical plane. Its azimuthal orientation had an irregular time dependence, but revealed a net azimuthal rotation with an average period of about 3 days for Rayleigh numbers $R > 10^{10}$. On average there was also a tendency for the LSC to be aligned with upflow to the west and downflow to the east, even after physically rotating the apparatus in the laboratory. The rate of azimuthal rotation and the probability distribution of the orientation of the LSC could be calculated from a model of diffusive azimuthal meandering in a potential due to the Earth's Coriolis force. This study revealed an additional contribution to the potential barrier that could be attributed to the cooling system of the sample top which dominated the preferred orientation of the LSC at

high R. The tendency for the LSC to be in a preferred orientation due to the Coriolis force could be cancelled by a slight tilt of the apparatus relative to gravity, although this tilt affected other aspects of the LSC that the Coriolis force did not.

10) Verzicco, R. (Bari)

A comparison of constant heat flux and constant temperature thermal convection

We numerically investigate turbulent thermal convection driven by a horizontal surface of constant heat flux and compare the results with those of constant temperature. Below $Ra \approx 10^9$, when the flow is smooth and regular, the heat transport in the two cases is essentially the same. For $Ra > 10^9$ the heat transport for imposed heat flux is smaller than that for constant temperature, and is close to experimental data. We provide a simple dimensional argument to show that the unsteady emission of thermal plumes renders typical experimental conditions closer to the constant heat flux case.

11) Benzi, R. (Rome)

TBA

12) Clercx, H.J.H. (Eindhoven)

Turbulent rotating convection - simulation and experiment

The turbulent motion of a fluid heated from below and cooled from above is currently the subject of many studies. In particular the convective heat transfer properties of the fluid are measured and theoretical predictions are tested to the results. A modification to this problem setting is the addition of a background rotation[1]. This modification is relevant in geophysical flows, e.g. convection in the atmosphere and the oceans[2]. The suppressing effect of rotation on the convective motion is best indicated through the Taylor-Proudman constraint: in a rapidly rotating fluid vertical variation in velocity is forbidden, leaving behind an essentially 2D flow. Linear stability theory predicts that at a high enough rotation rate all convective motion will have ceased and a static, purely conductive state remains[3]. Because of the rotational constraint the
flow-structuring in rotating convection is remarkably different from non-rotating convection. The motion is mostly confined to columns connecting top and bottom boundary layers, the flow inside these columns being strongly vortical due to spin-up of the converging boundary flow feeding the columns.
We are studying this flow setting in two ways. Experiments are conducted in a cylindrical convection cell, where velocity measurements are carried out with stereo-PIV. Additionally, direct numerical simulations (DNS) on both cylindrical and double-periodic domains provide reference data to compare to the experiment and to large-aspect-ratio convective systems like the atmosphere.
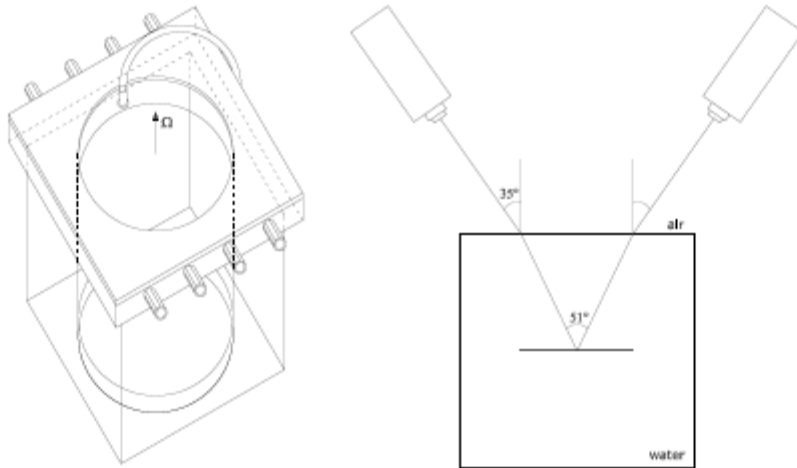
Figure 1: Sketches of the experimental set-up and camera positioning. The cylinder is surrounded by a square tank that is also filled with water to facilitate optical access. On the top the hollow lid (with temperature sensor) is shown, through which cooling water is circulated.

[1]H.T. Rossby, J. Fluid Mech. 36, 309{337 (1969).
[2]A.E. Gill, Atmosphere-Ocean Dynamics, Academic Press (1982).
[3]S. Chandrasekhar, Hydrodynamic and Hydromagnetic Stability, Oxford University Press (1961).
[4] M. Sprague et al., J. Fluid Mech. 551, 141{174 (2006).

The experimental set-up consists of a closed unit-aspect-ratio cylinder filled with water (figure 1). Seeding particles are added to the fluid. A laser illuminates a horizontal cross-section of the cylinder. Two cameras above the cylinder, with off_-axis angles, record the particle motion in this plane, providing full 3D velocity data there (figure 2). All of this equipment, as well as cooling and heating units for the cylinder, are positioned on a rotating table. The focal points of the experiments are: (a) the effect of a (small) background rotation on the large-scale circulation found in nonrotating high-Rayleigh-number convection, (b) the spatial distribution of the vortical columns at higher rotation rates, and (c) statistics of turbulence intensities. DNS is mainly used to investigate heat transfer (figure 3) and coherent structures that appear in the rotating-convective flow. The influence of the cylindrical sidewall is of interest, as well as a direct comparison between simulation and experiment. Of our prime interest are (a) the dependence of the heat transfer on the rotation rate, as well as (b) the internal structure of the coherent vortices that account for most of the heat transport, and (c) scaling of statistical quantities with rotation.
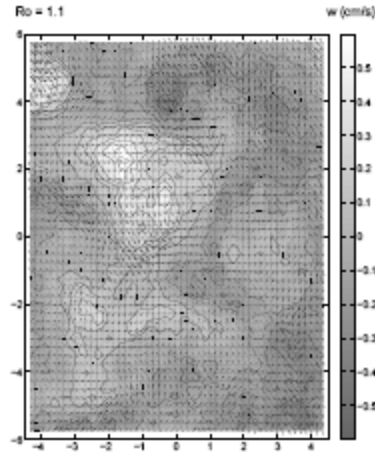
Figure 2: Three-component stereo-PIV velocity snapshot of an experiment. Arrows are for horizontal velocities, while contours and grey levels give the vertical velocity. Contour increment is 0.1 cm/s.
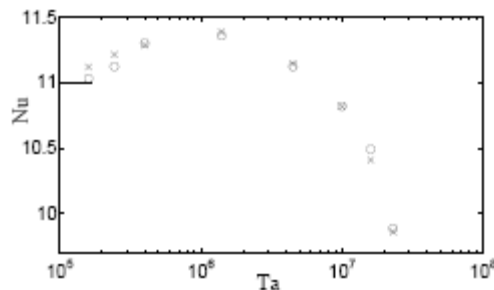

Figure 3: Heat transfer, denoted by the Nusselt number Nu, *from double-periodic DNS at different rotation rates (Taylor numbers* Ta*). The thick line on the axis indicates the heat transfer for* Ta = 0.

13) Ahlers, G. (Santa Barbara)

Recent experiments on turbulent RBC by the Santa Barbara group

Since Euromech 443 in Leiden three years ago our group (Denis Funfschilling, Eric Brown, Alexei Nikolaenko, and I) worked on the following:

1.) Precision measurements of turbulent heat transport in the range $10^7 < R < 10^{12}$ for Prandtl numbers near 4. This work was published as follows:
"Heat transport in turbulent Rayleigh-Bénard convection: Effect of finite top- and bottom-plate conductivity", E. Brown, A. Nikolaenko, D. Funfschilling, and G. Ahlers, Phys. Fluids 17, 075108 (2005).
"Heat transport by turbulent Rayleigh-Bénard Convection in cylindrical cells with aspect ratio one and less", A. Nikolaenko, E. Brown, D. Funfschilling, and G. Ahlers, J. Fluid Mech. 523, 251 (2005).
"Heat transport by turbulent Rayleigh-Bénard Convection in cylindrical cells with aspect ratio one and larger", D. Funfschilling, E. Brown, A. Nikolaenko, and G. Ahlers, J. Fluid Mech. 536, 145 (2005).

2.) The effect of tilting a cylindrical sample on turbulent heat transport, and on the Reynolds

number of the large-scale circulation (LSC). This work was published as:
"Search for slow transients, and the effect of imperfect vertical alignment, in turbulent Rayleigh-Bénard convection", G. Ahlers, E. Brown, A. Nikolaenko, J. Fluid Mech. 557, 347 (2006)

3.) Non-Boussinesq effects on the heat transport and Reynolds number in cylindrical Rayleigh-Bénard samples of water. This is a collaboration with the Twente/Marburg group and will be published as:
 "Non-Oberbeck-Boussinesq effects in strongly turbulent Rayleigh-Bénard convection", G. Ahlers, E. Brown, F. Fontenele Araujo, D. Funfschilling, S. Grossmann, and D. Lohse, J. Fluid Mech., in press.

4.) Aspect-ratio and Prandtl-number dependence of plume motion and large-scale circulation in cylindrical Rayleigh-Bénard samples. Much of this work has not yet been published. Denis Funfschilling will report on this topic on Wednesday morning.

5.) Effect of the Earth's Coriolis force on the large-scale circulation in cylindrical Rayleigh-Bénard samples. Eric Brown reported on this topic yesterday morning. This work has been submitted as
"Effect of the Earth's Coriolis force on the large-scale circulation of turbulent Rayleigh-Bénard convection", E. Brown and G. Ahlers, Phys. Fluids, submitted.

6.) Re-orientation of the large-scale circulation in cylindrical Rayleigh-Bénard samples. This work was published as:
"Orientation changes of the large-scale circulation in turbulent Rayleigh-Bénard convection", E. Brown, A. Nikolaenko, and G. Ahlers, Phys. Rev. Lett. 95, 084503 (2005).
"Rotations and cessations of the large-scale circulation in turbulent Rayleigh-Bénard convection", E. Brown and G. Ahlers, J. Fluid Mech., in press.

7.) Turbulent heat transport in compressed gases. This work is as yet unpublished.

In the remainder of this talk I will give a brief summary of topics 6.) and 7.):

6.) We made a broad range of measurements of the angular orientation $\theta_0(t)$ of the large-scale circulation (LSC) of turbulent Rayleigh-Bénard convection as a function of time. We used two cylindrical samples of different overall sizes, but each with its diameter nearly equal to its height. The fluid was water with a Prandtl number of 4.38. The time series $\theta_0(t)$ consisted of meanderings similar to a diffusive process, but in addition contained large and irregular spontaneous reorientation events through angles $\Delta\theta$. We found that reorientations can occur by two distinct mechanisms. One consists of a rotation of the circulation plane without any major reduction of the circulation strength. The other involves a cessation of the circulation, followed by a restart in a randomly chosen new direction. Rotations occurred an order of magnitude more frequently than cessations. Rotations occurred with a monotonically decreasing probability distribution $p(\Delta\theta)$, i.e. there was no dominant value of $\Delta\theta$ and small $\Delta\theta$ were more common than large ones. For cessations $p(\Delta\theta)$ was uniform, suggesting that information of $\theta_0(t)$ before the cessation is lost. Both rotations and cessations had Poissonian statistics in time, and occurred at any $\theta_0(t)$. The average azimuthal rotation rate $\langle d\theta_0(t)/dt \rangle$ increased as the circulation strength of the LSC decreased. Tilting the sample relative to gravity significantly reduced the frequency of occurrence of both rotations and cessations.

7.) The advantages of compressed gases for the study of Rayleigh-Bénard turbulence have been emphasized by numerous investigators. Changing the pressure or mean temperature permits the exploration of a different range of the Rayleigh number R without changing the geometry of the sample. Particularly near the critical point of a gas exceptionally large values of R can be attained (the disadvantages are mentioned less frequently: the conductivity is small and thus the nonlinear side-wall effects are relatively large). We chose ethane for our work because its equation of state is known exceptionally well. We found an increase of the Nusselt number due to non-Oberbeck-Boussinesq (NOB) effects that reached about 2% (6%) when the expansion coefficient times the temperature difference reached a value of about 0.1 (0.2). This differs qualitatively from the NOB effects in water, where the NOB Nusselt number was reduced below the Boussinesq value.

All of our papers and preprints may be found at
http://www.nls.physics.ucsb.edu/group_pub.html

14) Pesch, W. (Bayreuth)

On complex patterns in Rayleigh-Benard convection with broken chiral symmetry

Rayleigh-Benard convection, driven by a vertical temperature gradient applied to a horizontal fluid layer, is a prime paradigm for pattern forming instabilities in nonequilibrium systems. If the Boussinesq symmetry is violated, one observes stable hexagons instead of stripe (roll) patterns at onset. Rotation about a vertical axis breaks chiral symmetry, while horizontal isotropy still holds. A typical consequence is domain chaos in the roll state at onset of convection (Kuppers-Lortz instability). It will be demonstrated that hexagons react differently to rotation. One observes defect turbulent or bursting dynamics, which can be well understood in terms of a complex Ginzburg-Landau equation [1].The chiral symmetry can also be broken through a uniformily rotating horizontal acceleration, which can be introduced by suitably shaking the convection cell. The ensuing competion of shear-flow and bouyancy driven instabilities leads to a variety of interesting new phenomena and in particular to Kuppers-Lortz like chaos [2].

[1] S. Madruga, H. Riecke and W. Pesch, Phys. Rev. Lett., 96 074501 (2006)
[2] W. Pesch, F. Busse and J. Tao , in preparation.

15) Bodenschatz, E. (Goettingen)

Defect turbulence in inclined layer convection

We report experiments on defect turbulent patterns observed in inclined layer thermal convection close to the onset of instability. We concentrate on two situation of defect turbulence. The first is undulation chaos where undulating convection rolls perpetually tear and reconnect by the motion of dislocations. The other is hexaroll chaos, where a drifting hexagonal pattern is spatio-temporally chaotic. In this case the topological objects describing

the dynamics are penta-hepta defects and complexes of short-lived dislocation pairs in the same mode of two of the three modes generating the hexaroll planform. We describe the statistics of the defect turbulence of both states and show that they can be quantitatively understood by rate equations.

16) Grossmann, S. (Marburg)

Analogies between thermal convection and shear flow: RB Nusselt number, TC torque, and pipe friction coefficient

We expose analogies between turbulence in a fluid heated from below (RB) and shear flows in Taylor-Couette (TC) as well as in pipe (P) geometries. The relevant fluxes J as well as the excess dissipation rates ε_w due to the wind or the transversal turbulent transport flow are identified in all these flows. This allows to extend the unifying theory, developed for heat transport in RB flow (S. Grossmann and Detlef Lohse, JFM 407, 27-56 (2000) and subsequent refinements), in order to analyze the torque versus the rotation Reynolds number R_1 data in TC flow and the friction coefficient data versus mean flow Reynolds number in P flow. In particular the dependence on geometrical parameters can be studied as for example on the radius ratio η in TC flow.

17) Sreenivasan, K. R. (Trieste)

Ruminations in convection

18) Roche, P.E. (Grenoble)

Recent progresses on the Ultimate Regime issue

19) Funfschilling, D. (Santa Barbara)

How is the Large Scale Flow influenced by the aspect-ratio in a cylindrical Rayleigh-Bénard cell?

In turbulent Rayleigh-Bénard convection the fluid develops a large-scale flow (LSF). The shadowgraph method is used to visualize the plumes, which are used as tracers. In aspect ratio $\Gamma = D/L = 1$ (D and L are the diameter and height of the cell respectively), the LSF consists of a single roll, oscillating with a well defined frequency [1]. For $\Gamma = 2$ and 3, the LSF still consists of a single roll but has no or negligible oscillations. Also, for these aspect ratio, the density of plumes (ratio of the area occupied by the plumes by the total area) shows

clear oscillations at a well defined frequency. This later observation gives new interest in the model of Villermaux [2]. It also evidence a transition in the hydrodynamic regime between Γ = 1 and Γ= 2.

[1] D. Funfschilling and G. Ahlers, Phys. Rev. Lett. **92**, 194502 (2004)
[2] E. Villermaux, Phys. Rev. Lett. **75**, 4618 (1995)

20) Calzavarini, E. , (Twente)

Homogeneous Rayleigh-Benard convection

We present numerical results from direct numerical simulations of the bulk of a Rayleigh-Bénard system obtained by replacing the thermal and kinetic boundary layers with periodic boundary conditions [1, 2]. We focus on dimensional analysis and on scaling of global observables respect to the Rayleigh (Ra) and Prandtl (Pr) numbers. We show that at moderately high Ra, ($> 10^5$) the system displays the same scaling relations expected for a real RB system (i.e. with boundary layers) in the very large Ra regime [4]. In particular the heat flux scales with Ra accordingly to the Nu ~Ra½ behavior, also known as Kraichnan regime, see [3, 5] and Fig.1. The scaling of the heat flux respect to Pr is also discussed. At smaller Ra number the behavior of the system is found to be dominated by a particular class of exact, separable, solutions of the three-dimensional Boussinesq's equations in a periodic domain that produces exponential bursting both on Nusselt, as shown in Fig.2, and on Reynolds number [6]. The main features of the temporal and the spatial dynamics of the temperature and velocity components in such a regime are addressed in detail.
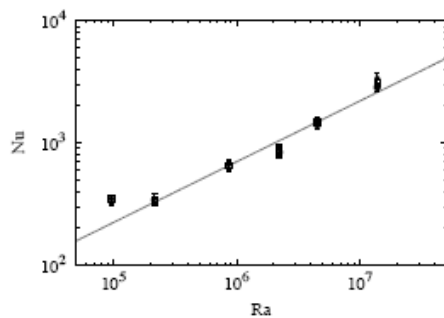

Figure 1: $Nu(Ra)$ for $Pr = 1$, computed in three different and independent ways ($\bullet$, $\square$ and $\circ$), see [5] for more details. The power law fit, performed on the mean value of the three different estimates and for $Ra > 10^5$, gives a slope 0.50 ± 0.05.
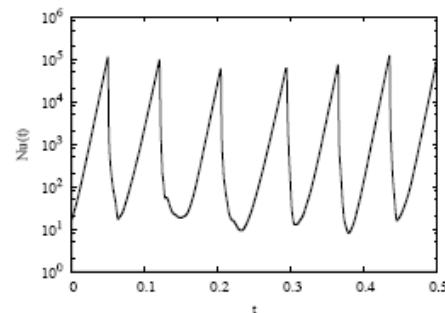
Figure 2: Time behavior of Nu at $Ra \simeq 2 \cdot 10^4$ and $Pr = 1$. Time is expressed in terms of the diffusive time across the cell, i.e. $t_d = H^2/\kappa$ where H is the height of the cell and κ the thermal diffusivity. The slope of the bursts is in agreement with the analytical solution.

References
[1] V. Borue and S. Orszag, (1997) J. Sci. Comp. 12, 305.
[2] D. Lohse and F. Toschi, (2003) Phys. Rev. Lett. 90, 034502.
[3] R. H. Kraichnan, (1962) Phys. Fluids 5, 1374.
[4] S. Grossmann and D. Lohse, (2000) J. Fluid. Mech. 407, 27.
[5] E. Calzavarini, D. Lohse, F. Toschi and R. Tripiccione,(2005) Phys. Fluid 17, 055107.

[6] E. Calzavarini, C. R. Doering, J. D. Gibbon, D. Lohse, A. Tanabe, and F. Toschi, (2006) Phys. Rev
E 73, 035301(R).

21) Toschi, F. (Rome)

Lagrangian Turbulence

22) Kunnen, R. (Eindhoven)

Rotational effects on turbulent convection

The classical Rayleigh-Benard setting consists of a layer of fluid that is enclosed between two horizontal parallel plates and heated from below. In a rotating frame of reference the flow dynamics change due to the presence of the Coriolis force. In many geophysical and astrophysical flow settings, e.g. atmospheric and oceanic convection, the combination of buoyancy and Coriolis forces largely determines the flow dynamics. We are investigating rotating Rayleigh-Benard convection with Direct Numerical Simulation (DNS). The current DNS code applies a finite-volume discretisation which is fourth-order accurate, solving the full Navier-Stokes equations including buoyancy and rotation under the Boussinesq approximation. At the top and bottom boundaries no-slip conditions are applied for velocity and the temperature is kept constant. Periodic boundary conditions in the horizontal directions make it possible to emulate a horizontally unbounded fluid layer, for example as a simple model for atmospheric convection. The effects of the rotation on global statistics and flow structuring are of our prime interest. In recent years the convective heat flux through a (nonrotating) fluid has been thoroughly studied. However, for the rotating case the picture changes; the heat flux depends in a remarkable way on the rotation rate, as is shown in figure 1(a). The convective plumes of turbulent convection are also affected by the rotation: the plumes are `spun up' as fluid converges to form a plume, which can be seen in figure 1(b). In upcoming simulations a cylindrical flow domain will be used. The results from those simulations are better suited for comparison with experiments. Also, the effect of the sidewall on heat flux and flow structuring can then be elucidated.
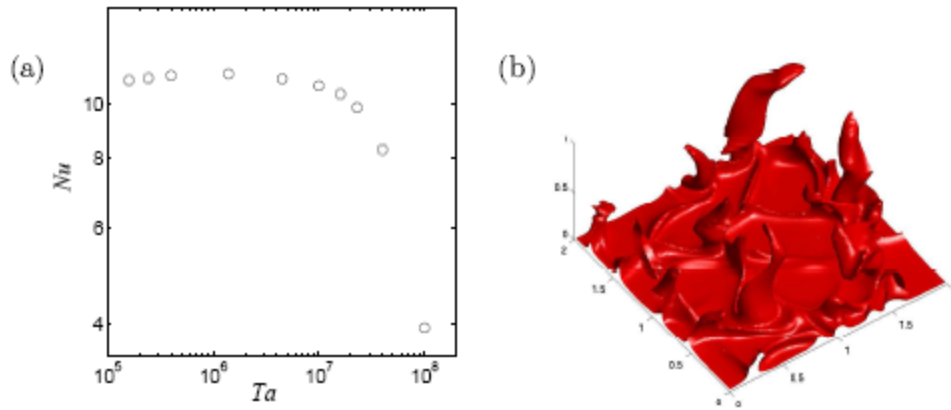
Figure 1: (a) The normalised heat flux (Nusselt number Nu) varies strongly with the scaled rotation rate (Taylor number Ta). Rayleigh number $Ra = 2.5 \times 10^6$, Prandtl number $\sigma = 1$. (b) Temperature isosurface plot showing the swirling effect of background rotation on the convective plumes.

23) Tilgner, A. (Goettingen)

Dissipation rates in Rayleigh-Benard convection

A central goal of research on Rayleigh-Benard convection is the prediction of the heat transport as a function of Rayleigh and Prandtl numbers. The heat transport is related to the dissipation rates of kinetic energy and temperature fluctuation. Estimates of these dissipation rates used in a theory proposed by Grossmann and Lohse have led to good predictions of the heat transport. However, measurements of the heat transport are a weak test of the theory as errors in the estimates for the dissipations could cancel each other. While dissipation is a quantity almost inaccessible to experiments, it can be easily extracted from numerical simulations. It is important to understand the scalings of dissipation rates before any theory based on them can be used to predict the heat transport for extreme values of the control parameters or in situations of geophysical relevance, which include rotation, shear, spherical geometry, or non uniform gravitational acceleration. This talk will present numerical results on Rayleigh-Benard convection and in particular on the dissipation occurring in these flows.

24) Steinberg, V., (Rehovot)

Strong non-Boussinesq effect in turbulent convection in a gas near the critical point

25) Breuer, M. (Muenster)

The validity of two-dimensional numerical approaches to time-dependent thermal convection

High resolution computer simulations of two-dimensional (2D) convection are often used to investigate turbulent flows. In this paper we compare numerical simulations in 2D with three-dimensional (3D) simulations. We investigate flows at a fixed Rayleigh number of $Ra=10^6$. The velocity boundary conditions are rigid for the upper and lower boundary and stress-free for the side walls. For high values of the Prandtl number the flow structure and global quantities such as the Nusselt number (Nu) and the Reynolds number (Re) show similar behaviour in 3D and 2D simulations. For values of the Prandtl number smaller than unity however the 2D results diverge strongly form the 3D findings. This is true not only for global properties (Nu, Re) but also for local properties such as the structure of the boundary layer and the shapes of the up- and down-wellings. We relate this behaviour to the different large-scale structure of the flow and the toroidal component of the kinetic energy.

26) Tong, P. (Hong Kong)

Spatial distribution of the local thermal dissipation rate in turbulent Rayleigh-Benard convection

The time-averaged local thermal dissipation rate $\varepsilon_T(r)$ is closely related to heat transport in turbulent thermal convection. In this talk, I will report results of a new experimental study of the spatial distribution and statistical properties of the measured $\varepsilon_T(r)$ in turbulent convection. The local thermal dissipation rate $\varepsilon_T(r)$ is obtained from simultaneous measurements of three components of the temperature gradient vector in cylindrical cells filled with water. It is found that the measured $\varepsilon_T(r)$ contains two contributions; one is generated by thermal plumes and occupies mainly in the plume-dominated bulk region. The other contribution comes from the mean temperature gradient and is concentrated in the thermal boundary layers. The experiment provides new insights into the mechanism of heat transport in turbulent convection.
*Work done in collaboration with X.-Z. He and K.-Q. Xia and was supported in part by the Research Grants Council of Hong Kong SAR.

27) Sugiyama, K., (Twente)

Numerical study on non-Oberbeck-Boussinesq effects in Rayleigh-Bernard convection

We investigate the Non-Oberbeck-Boussinesq (NOB) effects in the two-dimensional Rayleigh-Benard turbulence for water and for glycerol. We perform direct numerical simulations, in which the temperature dependences of the viscosity, the thermal diffusivity and the thermal expansion coefficient are fully considered. We focus on the temperature profiles, the center temperature T_c, and the deviation from the Oberbeck-Boussinesq (OB) Nusselt number $Nu_{NOB}=Nu_{OB}$. We vary the Rayleigh number Ra (up to 10^8 for water and

10^7 for glycerol) and the temperature difference (up to 60K) between top and bottom plates. Our numerical results of Tc and $Nu_{NOB}=N_{uOB}$ are consistent with the available experimental data (e.g. see Fig. 1). In addition, we find that Tc is well predicted by the Prandtl-Blasius Boundary layer theory [1] and weakly dependent on Ra for fixed Δ. To quantify the physical mechanism to alter the Nusselt number from the OB to the NOB for fixed Ra and Δ , we decompose the Nusselt number ratio $Nu_{NOB}=N_{uOB}$ as the product of two effects: (1) the change of the thermal boundary layer thickness and (2) the changes of Tc and thermal diffusivity at top and bottom walls. This decomposition indicates that while for glycerol $Nu_{NOB}=N_{uOB}$ is governed by the first effect, for water it is by the second one.
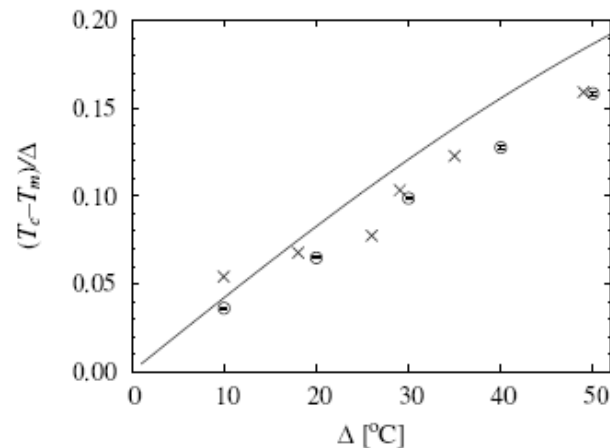

Figure 1: The normalized deviation of the center temperature $(T_c - T_m)/\Delta$ versus the temperature difference Δ for glycerol. The mean temperature T_m between the top and bottom plates is fixed at 40°C. The symbol ∘ shows the present DNS at $Ra = 10^7$. The symbol × shows the experimental data [2]. The line shows the prediction by the Prandtl-Blasius Boundary layer theory [1].

References
[1] Ahlers, G., Brown, E., Fontenele Araujo, F., Funfschilling, D., Grossmann, S. and Lohse, D.,
2006, Non-Oberbeck-Boussinesq e_ects in strongly turbulent Rayleigh-B_enard convection, J. Fluid Mech. (submitted).
[2] Zhang, J., Childress, S. and Libchaber, A., 1997, Non-Boussinesq e_ect: Thermal convection
with broken symmetry, Phys. Fluids, 9, 1034-1042.

28) Abarzhi, S. (Chicago)

TBA

29) Glatzmaier, G. (Santa Cruz)

Numerical simulations of rotating convection in density-stratified electrically-conducting fluids

Thermal convection in the deep fluid interiors of planets and stars is dominated by the effects of rotation. The dynamics in the liquid iron cores of terrestrial planets are also influenced by strong Lorentz forces. Large stratifications of density further complicate turbulent

convection in the interiors of giant planets and stars. A series of computer simulations, both 2D and 3D, will be presented illustrating the progress made toward understanding these flows. Hopefully these results will inspire new laboratory experiments that will guide and validate the numerical simulations as they become more turbulent.

30) Hansen, U. (Muenster)

Steady-state and turbulent convection: similarities and distinctions

Convection is the primary transport mechanism in the rocky mantle of planets, in particular in the Earth. Due to the high viscosity of the material, this type of convection is characterized by an infinite Prandtl number (no inertia). While advective transport of momentum is not important, advection strongly dominates the transport of heat, i.e. the Rayleigh number is high. Under this circumstances convection typically emerges as highly time dependent, chaotic flow, consisting of a large scale wind with superimposed small-scale instabilities. Besides temporal fluctuations due to the small scale instabilities, variations of the large scale flow are also observed (e.g. flow reversals). However, also stationary solutions can numerically be obtained, describing a steady-state flow. For 2D-flow, under stress-free boundary conditions, the Nusselt number of the chaotic flow can be shown to represent a Gaussian distribution with the same mean value, as obtained from the stationary solution. Since the stationary solutions can be calculated relatively fast, it allows for a systematic investigation of scaling laws, specially the relation between Nusselt- and Rayleigh number . For an aspect ratio of unity the theoretically predicted values of the exponents of 1/3 (stress-free) and 1/5 (rigid boundaries) in the Nu-Ra relation are found. The Nusselt Number is further strongly dependent on the aspect ratio of the circulation and so is the exponent in the Nu-Ra relation. In general the exponents decrease with increasing aspect ratio and vice versa. Numerical experiments in small slots reveal exponents being significantly larger than 1/3.

31)   Tsai, P. (Toronto)

Charge transport scaling in turbulent electroconvection

We present measurements of the normalized charge transport, or electric Nusselt number Nu, as a function fluid parameters for turbulent convection in an electrically driven thin film. The experimental system consists of a weakly conducting, submicron-thick liquid crystal film suspended between concentric circular electrodes. The film develops a surface charge configuration that is unstable to the applied voltage. This situation is analogous to the inverted fluid density distribution which is unstable to the buoyancy force in thermal convection. Under a large applied voltage, approximately a hundred times larger than the critical voltage at the onset of convection, the flow is unsteady and electric charge is turbulently transported between electrodes.   There are three important dimensionless parameters, analogous to those of Rayleigh-B\'{e}nard convection: a Rayleigh-like number, R, that describes the intensity of forcing and is proportional to the square of the applied voltage V^2. A Prandtl-like number, P, which is the ratio of charge relaxation time to viscous relaxation time. Finally, the aspect ratio Γ, or radius ratio, characterizes the annular geometry. Our experimental data show local $Nu-R$ scalings, $Nu \sim R^r$, where the scaling exponents r were either 0.20 ± 0.03 or 0.25 ± 0.02, for $10^4 \leq R < \leq 2 \times 10^5$, with Γ ranging from 0.3 to 17 and for P ranging from

5 to 250. To investigate further the Nu-R scaling, we develop a scaling theory which closely parallels the Grossmann-Lohse model and predicts the local power law $Nu \sim F(\Gamma) R^r P^\beta$. The dimensionless function $F(\Gamma)$, which emerges as an outcome of the scaling theory, describes the dependence of Nu on the aspect ratio Γ of the annulus. We find that our experimental measurements of Nu are consistent with the scaling theory. In spite of the general consistency between the experiment and theory, it is difficult to draw definitive conclusions about the validity of the assumptions underlying the scaling theory. The decomposition of the dissipation into various contributions, which is a key assumption of the theory, is not directly testable with our current experimental techniques. To attack this deficiency, we have developed a realistic direct numerical simulation code. These simulations complement the experimental study by providing access to the complete stream function, charge and electric potential fields. We present our preliminary simulation results on the sequence of bifurcations leading to turbulent electroconvection and the scaling regime.

32) Kerr. R, (Warwick)

Direct numerical simulations of three-dimensional thermohaline fingering and fluxes

Three-dimensional Direct Numerical Simulations (DNS) of the salt fingering regime are described and shown to be applicable to the ocean. At high resolution ($512 \times 512 \times 128$) for a low density ratio of $R_{\rho} = 1.2$, fingers appear spontaneously from smooth initial conditions. With small scale seeding, similar results are found in smaller calculations ($64 \times 64 \times 256$), allowing several cases to be simulated and trends with R_ρ to be determined.

These show a rapid decrease in the net salt diffusivity, K_S% from order $1 \sim {\rm cm}^2/{\rm s}$ to $0.01 \sim {\rm cm}^2/{\rm s}$ as R_{ρ} increases from 1.2 to 2.0. Fingering layers form on interfaces during an early stage if R_ρ is small and there is a large-scale perturbation. The statistical state at late times for lower R_ρ is a sea of vertically oriented fingers without staircases and is independent of the initial condition. These trends are consistent with oceanic observations and support a widely use ocean parametrization of double diffusion.

33) King, M. (U. Alaska)

Preliminary results for 2D simulation of convection in a rotating annulus

Bohn et al (1995) performed heat transfer measurements in rotating annuli with heated outer rim and cooled inner rim for 7<=lg(Ra)<=11. The range of the values for the exponent (in Nu ~ Ra^\gamma) obtained were around 0.21 to 0.23 for the annuli with different aspect ratios that were used. I will discuss preliminary results from 2D direct numerical simulations that I have performed and which appear to produce a similar exponent of 0.23+-0.01. Possible explanation for the results using RB convection theory may be suggested.

34) van Reeuwijk, M. (Delft)

Wind and its boundary layers in Rayleigh-Benard convection

The turbulent wind of Rayleigh-B\'{e}nard convection and its effect on the boundary layers is studied by direct numerical simulation in an aspect-ratio 4 domain with periodic sidewalls at Ra= 10^5, 10^6, 10^7 and at Pr=1. Symmetry-accounting ensemble-averaging has been applied to decompose independent realizations into wind and fluctuations. It is shown that the characteristic peak in the squared mean horizontal velocities by which the hydrodynamic boundary layer thickness is approximated, is nearly entirely due to the wind. Both the wind and the fluctuations scale approximately at Re ~ Ra^0.5.

From a study of the momentum and temperature budgets it follows that the boundary layers are clearly turbulent, although standard turbulence indicators like the shape factor and friction factor point towards laminarity. Overall, it is found that buoyancy forces significantly alter the structure of the boundary layer, and can therefore not be neglected in its characterization and parametrization.

35) Thess., A. (Ilmenau)

Structure of the thermal boundary layers in turbulent Rayleigh-Benard convection

It is well known that the profile of the mean temperature in turbulent Rayleigh-Benard convection consists of a diffusive (linear) zone in the vicinity of the heating and cooling plates, a near-constant temperature zone in the bulk far away from the plates, and a nonlinear zone between these two. Various phenomenological predictions exist for the shape of the temperature profile in the nonlinear zone including Prandtl's classical -1/3 scaling, logarithmic scaling and power law scaling. Since the spatial resolution of temperature measurements was limited in previous experiments, it was difficult to decide which of the phenomelogical models is correct. We report temperature measurements with high spatial resolution performed in a large-scale Rayleigh-Benard facility with air. The measurements suggest a power law scaling of the mean temperature field near the upper (cooling) plate. Future measurements using a new heating plate with improved thermal homogeneity will be briefly discussed.

36) Arakeri, J. H. (Bangalore)

From convection in a closed cavity, Nu~Ra**1/3 limit, to convection in an open ended cavity, Nu~Ra**1/2 limit

This talk addresses turbulent convection in two types of cavities. One is the standard Rayleigh Benard (RB) convection where the top and bottom ends of cavity are closed and where Nu~Ra$^{1/3}$. (Nu and Ra are Nusselt number and Raleigh number respectively). In the

second type of the top and bottom ends of the cavity are open and where we find $Nu \sim Ra^{1/2}$. In both cases convection is caused by an unstable vertical density difference.

In RB convection, we discuss a plume model for the near-wall flow, the role of the wind, propose an experimental technique to study high Ra, high Prandtl number (Pr) convection, and propose a Cf type non-dimensional representation for heat flux. It is well known that the near wall flow consists of randomly moving line or sheet plumes. Akin to Howard's thermal model, we have a model for the plumes from which we get the average plume spacing, and near wall distributions of mean temperature and rms of temperature and velocity fluctuations. The model [2] is based on the following conjecture: each plume has associated with it two boundary layers on either side: boundary layer becoming unstable at some critical Ra leads to plume formation. This instability determines the plume spacing. For $Pr \approx 1$, the model predicts that the average plume in given by $Ra_\lambda^{1/3} \approx 50$, where Ra_λ is Rayleigh number based on plume spacing. Experimental results are in agreement with model predictions [2, 3]

The new experimental technique [4] to obtain high Rayliegh number ($\sim 10^{''}$) and high Prandtl number (~ 1000) turbulent convection, uses brine diffusing across a micro-porous membrane. The low diffusivity of the salt gives the high Ra and Pr. As in $Pr \sim 1$ convection, the near wall is dominated by sheet plumes. The non-dimensional plume spacing $Ra_\lambda^{1/3} \approx 90$ for this higher Pr. The measured plume spacings show a lognormal distribution [4].

What is the role of the outer flow (or the wind)? As suggested by the $Ra^{1/3}$ scaling, the outer flow has little influence on the heat flux. The main effect is that the wind aligns the plumes in the flow direction [3, 4]. In fact, the wind leaves a clear signature on the near wall plume structure.

We propose an alternate non-dimensionalization of heat flux, which for turbulent convection is more appropriate than Nusselt number. This alternate representation is analogous to the C_f representation for wall stear stress and removes the length scale that is present in Nu.

Removing the bottom and top walls, i.e., convection in an open-ended vertical cavity results in a completely new type of flow:

1. $Nu \sim (RaPr)^{1/2}$; heat flux is independent of molecular diffusive properties kinematic viscosity (γ) and thermal diffusivity (α).

2. In a tall enough cavity we obtain an *axially homogenous purely buoyancy driven turbulence in the presence of a linear (unstable) density gradient*. This flow is the free convection analog of fully developed pipe flow driven by a linear pressure gradient.

3. Much higher fluxes and Reynolds numbers are obtained than those obtained in RB convection for the same temperature difference and apparatus size.

We propose a model for the flux, and present the structure of the flow in terms velocity fluctuations, PDFs and spatial correlations[6,7,8].

REFERENCES:

1. Theerthan, S.A & J.H. Arakeri, 1994, "Plan form structure of turbulent Rayleigh – Benard convection". Intl Commun. Heat Mass Transfer 21, 561-572.

2. Theerthan, S.A & J.H. Arakeri, 1998, "A model for near wall dynamics in turbulent Rayleigh Benard convection". J. Fluid. Mech. 373, 221-254.

3. Theerthan, S.A & J.H. Arakeri, 2000, "Plan form structure and heat transfer in turbulent free convection over horizontal surfaces", Phys. Fluids, 12, 884-894.

4. Puthenveettil B.A., & J.H. Arakeri, 2005, "Plume structure in high-Rayleigh number convection", J. Fluid. Mech. , Vol. 542, pp. 217-249.

5. Puthenveettil, B.A & J.H. Arakeri, 2005, "Multifractal nature of plume structure in high Rayleigh number convection". J. Fluid. Mech. 526, 245-256.

6. Jaywant H Arakeri, F.E Avila, J.M. Dada, & R.O. Tovar, 2000, "Convection in a long vertical tube due to unstable stratification – a new type of turbulent flow"? Current Sci. 79 (6) 859-866.

7. Murali R. Cholemari & Jaywant H Arakeri, 2005, "Experiments and a model of turbulent exchange flow in a vertical pipe", International Journal of Heat & Mass Transfer 48, 4467-4473.

8. M.R. Cholemari, "Buoyancy driven turbulence in a vertical pipe, Ph.D. thesis", Department of Mechanical Engineering, Indian Institute of Science, 2004.